

Bag of Baselines for Multi-objective Joint Neural Architecture Search and Hyperparameter Optimization

Julia Guerrero-Viu

GUERRERO@CS.UNI-FREIBURG.DE

Sven Hauns

HAUNSS@TF.UNI-FREIBURG.DE

Sergio Izquierdo

IZQUIERD@CS.UNI-FREIBURG.DE

Guilherme Miotto

ALESSANG@CS.UNI-FREIBURG.DE

Simon Schrodi

SCHRODI@CS.UNI-FREIBURG.DE

André Biedenkapp

BIEDENKA@CS.UNI-FREIBURG.DE

University of Freiburg

Thomas Elsken

THOMAS.ELSKEN@DE.BOSCH.COM

Bosch Center for Artificial Intelligence

Difan Deng

DENG@TNT.UNI-HANNOVER.DE

Marius Lindauer

LINDAUER@TNT.UNI-HANNOVER.DE

Leibniz University Hannover

Frank Hutter

FH@CS.UNI-FREIBURG.DE

University of Freiburg and Bosch Center for Artificial Intelligence

Abstract

Neural architecture search (NAS) and hyperparameter optimization (HPO) make deep learning accessible to non-experts by automatically finding the architecture of the deep neural network to use and tuning the hyperparameters of the used training pipeline. While both NAS and HPO have been studied extensively in recent years, NAS methods typically assume fixed hyperparameters and vice versa — there exists little work on joint NAS + HPO. Furthermore, NAS has recently often been framed as a multi-objective optimization problem, in order to take, e.g., resource requirements into account. In this paper, we propose a set of methods that extend current approaches to jointly optimize neural architectures and hyperparameters with respect to multiple objectives. We hope that these methods will serve as simple baselines for future research on multi-objective joint NAS + HPO. To facilitate this, all our code is available at <https://github.com/automl/multi-obj-baselines>.

1. Introduction

Neural architecture search (NAS) (Zoph and Le, 2017; Elsken et al., 2019b; Wistuba et al., 2019) and hyperparameter optimization (HPO) (Feurer and Hutter, 2019) make deep learning accessible to non-experts by automatically tuning the employed neural network architecture and the hyperparameters of a deep learning algorithm.

While both fields have been studied extensively in recent years, NAS methods typically assume fixed hyperparameter configurations and vice versa.¹ There exists little work on *jointly* optimizing hyperparameter configurations and neural network architectures (Zela et al., 2018; Dong et al., 2020; Zimmer et al., 2021), even though it seems natural that

1. HPO methods sometimes also consider some architectural hyperparameters but often specialize in optimizing (few) continuous hyperparameters rather than the discrete choices characteristic of NAS.

Proposed Method	Based on	Extended by
SH-EMOA (Sec. 3.1)	multi. obj. evolution	successive halving
MO-BOHB (Sec. 3.2)	BOHB	multi-objective for candidate selection, MOTPE
MS-EHVI (Sec. 3.3)	BO with EHVI	no surrogate for cheap objectives
MO-BANANAS (Sec. 3.4)	BANANAS	multi-objective candidate selection, successive halving
BULK & CUT (Sec. 3.5)	EA, BO	network morphism, pruning with knowledge distillation, constrained BO

Table 1: Overview of the proposed methods.

different architectures require different hyperparameter configurations to yield optimal performance. Indeed, there is evidence that this is actually the case.

For example, Gastaldi (2017) showed that the strongest version of the proposed shake-shake regularization performs best for some architectures, but is too strong for other architectures, resulting in poor performance or even divergence during training. Thus, a joint optimization of hyperparameter configurations and architecture can be expected to be beneficial.

While NAS and HPO methods typically optimize for accuracy, in many real-world applications there is more than one objective. Common objectives next to accuracy are, e.g., memory requirements, energy consumption or latency on the target hardware where the neural network is eventually deployed.

In this paper, we take a first step in the direction of *multi-objective joint NAS + HPO* by proposing and empirically evaluating a set of simple, yet powerful baseline methods. All our baseline methods essentially extend current NAS or HPO approaches to cover both classical and architectural hyperparameters, optimized under multiple objectives; see Table 1 for an overview of the methods we propose.

2. Related Work and Background

Neural Architecture Search (NAS). NAS refers to the task of automatically learning neural network architectures from data (Elsken et al., 2019b). NAS approaches often employ black-box optimization methods, such as evolutionary algorithms (Real et al., 2017, 2019), reinforcement learning (Zoph and Le, 2017), or Bayesian optimization (Mendoza et al., 2016; Kandasamy et al., 2018; White et al., 2019). However, due to the large computational costs, researchers have developed methods tailored towards NAS, e.g., (gradient-based) optimization on one-shot models (Bender et al., 2018; Pham et al., 2018; Liu et al., 2019).

Hyperparameter Optimization (HPO). It is widely acknowledged that tuned hyperparameter configurations can improve the performance of machine learning models. Tuning manually, however, is a tedious and error-prone task. The field of HPO (see e.g., Feurer and Hutter, 2019, for an overview) automates the search for well performing hyperparameter configurations for the data at hand. Commonly, HPO is treated as a black-box optimization. Bayesian Optimization (BO) (Brochu et al., 2010; Shahriari et al., 2016) is a popular framework for global optimization of expensive black-box functions and has shown great success in HPO (see e.g., Snoek et al., 2012, 2014; Feurer et al., 2015; Springenberg et al., 2016; Eriksson et al., 2019; Kandasamy et al., 2020). BO models the expensive function using a cheap-to-evaluate probabilistic surrogate model and uses an acquisition function to trade-

off exploration and exploitation for selecting a new candidate point. Gaussian Processes (GP) (Rasmussen and Williams, 2006) and expected improvement (EI) (Moćkus, 1975) are the most common choices for these. The tree-structured parzen estimator (TPE) (Bergstra et al., 2011) is an alternative surrogate that models density functions of good and bad hyperparameter configurations, respectively; optimizing the ratio of these densities is equivalent to optimizing EI (Bergstra et al., 2011).

Multi-fidelity Optimization. As fully training and evaluating ML pipelines (e.g., deep neural networks) can be too expensive to evaluate many configurations, multi-fidelity methods employ cheaper fidelities to reduce this cost, e.g., training only on a small subset of the data (Klein et al., 2017) or for a few epochs (Falkner et al., 2018). Successive Halving (SH) (Jamieson and Talwalkar, 2016) and Hyperband (HB) (Li et al., 2018) are two powerful multi-fidelity strategies that allocate more budgets on the well-performing hyperparameter configurations and achieve strong anytime performance. However, both strategies select new hyperparameter configuration at random without exploiting the knowledge gained about well-performing regions. BOHB (Falkner et al., 2018), which combines BO and HB, overcomes this issue by introducing a TPE model into Hyperband to guide the search.

Joint NAS + HPO. Few researchers so far have considered the joint optimization of architectures and hyperparameter configurations. Domhan et al. (2015) and Mendoza et al. (2016) used the random-forest-based blackbox BO method SMAC (Hutter et al., 2011) to jointly optimize both architectures and hyperparameter configurations (e.g., number of filters, number of layers/blocks, and conditional layer hyperparameters that are only active if a layer exists). Zela et al. (2018), Runge et al. (2019) and Zimmer et al. (2021) employed the more efficient multi-fidelity method BOHB (Falkner et al., 2018) to achieve the same goal. Saikia et al. (2019) first employ DARTS (Liu et al., 2019) to search for better architectures for the task of disparity estimation and then optimize the hyperparameters of the resulting architecture with BOHB. Finally, Dong et al. (2020) extended NAS methods using one-shot models to also consider hyperparameters.

Multi-objective Optimization Multi-objective optimization (e.g., Miettinen (1999)) deals with the problem of minimizing multiple objective functions $f_1(\lambda), \dots, f_n(\lambda)$. In general, there is no single λ that minimizes all objectives at the same time since the objectives are often in competition with each other. Rather, there are multiple *Pareto-optimal* solutions that are optimal in the sense that one cannot reduce any f_i without increasing at least one other f_j ($i \neq j$). The set of Pareto-optimal solutions is called the *Pareto front*.

Multi-objective Optimization with Evolutionary Algorithms. One class of algorithms for solving multi-objective problems are evolutionary algorithms, e.g., Deb (2015). Criteria for selecting candidates being mutated and defining the best current solutions are typically based on *non-dominated sorting* (NDS) (Srinivas and Deb, 1994; Deb et al., 2002) and the *hypervolume indicator* (Emmerich et al., 2005; Beume et al., 2007; Bader and Zitzler, 2011); we describe these techniques in the following.

NDS extends the ranking of a set of candidates based on a single objective to multiple objectives $f = (f_1, \dots, f_n)$ in the following way:

- Compute the Pareto front $\mathcal{F}_1 = \text{pareto_front}(\mathcal{P}|f)$ of the current population \mathcal{P} and assign all members of this Pareto front \mathcal{F}_1 the best rank.

- Remove the previous Pareto front from the population \mathcal{P} and compute the Pareto front for the remaining population: $\mathcal{F}_2 = \text{pareto_front}(\mathcal{P} \setminus \mathcal{F}_1 | f)$. Members of this new Pareto front \mathcal{F}_2 are assigned the second best rank.
- Iterate this process until all members of the population have been assigned a rank.

Thus, a run of NDS partitions the population into sets $\mathcal{F}_1, \dots, \mathcal{F}_k$, where a candidate $\lambda \in \mathcal{F}_i$ outperforms another candidate $\lambda' \in \mathcal{F}_j$ with respect to all objectives if $i < j$.

The *hypervolume indicator* I_H of a population measures, informally speaking, the space of objective function values covered by the population; maximizing the hypervolume indicator corresponds to improving the Pareto front and finding better solutions. Based on the hypervolume indicator, the *hypervolume subset selection problem* (HSSP) (Bader and Zitzler, 2011) is defined as the problem of finding a subset $\mathcal{P}_{HSSP} \subset \mathcal{P}$ of a certain size k so that the hypervolume is maximized for this subset: $\mathcal{P}_{HSSP} \in \arg \max_{\mathcal{P}' \subset \mathcal{P}, |\mathcal{P}'|=k} I_H(\mathcal{P}')$. The HSSP can also be solved to identify a poorly performing candidate by setting $k = |\mathcal{P}| - 1$ and choosing the poor candidate λ_{poor} as the one that gets removed from the population via HSSP: $\{\lambda_{poor}\} = \mathcal{P} \setminus \mathcal{P}_{HSSP}$. We refer to Bader and Zitzler (2011) for a more formal introduction.

Multi-objective Optimization with Bayesian Optimization (BO). Traditional BO approaches only consider single objectives. However, extending BO to the multi-objective case only requires a few modifications. For example, similar to how EI considers improvements of the objective based on a surrogate, Expected Hypervolume Improvement (EHVI) (Emmerich, 2005) considers contributions to the Pareto front based on a surrogate function. EHVI has become a widely used acquisition function for multi-criteria problems due to recent works reducing the computation overhead for its calculation (Yang et al., 2019; Daulton et al., 2020). Recently, Ozaki et al. (2020) also extended TPE to multi-objective TPE (MOTPE) by using EHVI

and a multi-objective splitting criterium to estimate the densities used in TPE.

Multi-objective and constrained NAS. *Hardware-aware* NAS has recently emerged as an important criterion for neural architectures, since many real-world applications require efficient architectures w.r.t., e.g., memory requirements, energy consumption or latency on the target hardware where the neural network is eventually deployed. Consequently, a line of research frames NAS either as a constrained (Tan et al., 2019; Cai et al., 2019) or multi-objective (Elsken et al., 2019a; Lu et al., 2019; Schorn et al., 2020) optimization problem to take this into account, we refer to Benmeziene et al. (2021) for a recent survey.

3. Proposed Methods

In the following, we propose five simple, yet powerful extensions of existing HPO and NAS optimization techniques to multi-objective joint HPO + NAS.

3.1 SH-EMOA: Speeding up Evolutionary Multi-Objective Algorithms

The flexibility and conceptual simplicity of evolutionary algorithms make them directly applicable to multi-objective optimization problems. For example, the well-known SMS-

EMOA from Beume et al. (2007) is an evolutionary algorithm that evaluates the performance of each candidate based on its contribution to the dominated hypervolume. Although effective, evolutionary algorithms tend to be very sample-inefficient, making them too computationally expensive for many practical applications. In order to deal with this problem, we propose **SH-EMOA** to speed up evolutionary multi-objective algorithms (EMOA) by using a multi-fidelity approach based on successive halving, see Algorithm 1.

After initializing the population, we iterate EMOA with doubling the training budgets in each iteration, while the number of candidates is halved. Thus, many candidates are evaluated with a small budget to cover a wide range of solutions, while only well-performing candidates proceed to the next stage, and are evaluated with the next higher budget and used to generate new candidates. The population size remains constant, so to remove a candidate from the population we first use non-dominated sorting (NDS) to identify the subset of the population with lowest rank and then solve the hypervolume subset selection problem (HSSP) on this lowest-rank subset to identify a poorly performing candidate, which is removed from the population.

Algorithm 1: SH-EMOA

Input : number of function evaluations n_{fe}^{total} , population size s_{pop} , maximum budget b_{max} , number of SH iterations n , objectives f

Output: Pareto front w.r.t. f

- 1 Generate initial population \mathcal{P} of size s_{pop}
- 2 $b \leftarrow \lfloor b_{max}/2^{n-1} \rfloor$ /* initial budget */
- 3 $n_{fe} \leftarrow \lfloor n_{fe}^{total} / \sum_{i=0}^{n-1} 2^{-i} \rfloor$ /* number of FE for the initial budget */
- 4 **for** $i = 1$ **to** n **do**
- 5 Evaluate $f(\lambda)$ for all $\lambda \in \mathcal{P}$ with budget b
- 6 **for** $j = 1$ **to** $n_{fe} - s_{pop}$ /* generate candidates for remaining FEs */
- 7 **do**
- 8 Generate new candidate λ_{new} /* parent selection and variation */
- 9 Evaluate $f(\lambda_{new})$ on budget b
- 10 $[\mathcal{F}_1, \dots, \mathcal{F}_k] \leftarrow \text{NDS}(\mathcal{P} \cup \{(\lambda_{new}, f(\lambda_{new}))\})$
- 11 $\lambda_{poor} \leftarrow \text{HSSP}(\mathcal{F}_k, |\mathcal{F}_k| - 1)$
- 12 $\mathcal{P} \leftarrow (\mathcal{P} \cup \{(\lambda_{new}, f(\lambda_{new}))\}) \setminus \{(\lambda_{poor}, f(\lambda_{poor}))\}$
- 13 $n_{fe} \leftarrow n_{fe}/2$ /* half number of FE in next budget */
- 14 $b \leftarrow 2b$ /* double budget */
- 15 **return** $pareto_front(\mathcal{P}|f)$

Even though **SH-EMOA** can be expected to require a high number of FEs, it is conceptually simple, flexible, and highly parallelizable.

3.2 MO-BOHB: Generalization of BOHB to an Arbitrary Number of Objectives

In order to extend BOHB (Falkner et al., 2018) to multi-objective optimization, we apply two changes, one related to the BO part and one related to the HB part. Firstly, we replace the TPE (Bergstra et al., 2011) originally used in BOHB by MOTPE (Ozaki et al., 2020) to

guide the search by selecting new configurations under consideration of multiple objectives. Secondly, we extend HB (Li et al., 2018) in a similar fashion as for SH-EMOA and MOTPE to decide with which configuration to proceed in the next stage: we use NDS and the result of the HSSP (Bader and Zitzler, 2011).

Our proposed MO-BOHB generalizes BOHB to an arbitrary number of objectives by making the aforementioned modifications; in particular, a single objective is only a special case. Note that this approach can also be used to extend to other methods combining a (multi-objective) black-box optimizer and multi-fidelity optimization strategy.

3.3 MS-EHVI: Mixed Surrogate Expected Hypervolume Improvement

Although EHVI (Emmerich, 2005) can be directly applied for joint NAS and HPO obtaining competent results, we further enhance the algorithm by a simple observation from Elsken et al. (2019a): while some of the objective functions are expensive to evaluate (e.g., evaluating the accuracy is expensive since it requires training the network first), other are cheap to evaluate (e.g., the number of parameters). Thus, rather than relying on a surrogate model for *every* objective function as in vanilla EHVI, we solely use surrogate models for the expensive objective function and directly evaluate the cheap objectives. This way, we avoid fitting surrogate models for objectives which are cheap to evaluate anyway and avoid poor predictions of the surrogate models.

We refer to Algorithm 2 for pseudo-code. The approach is very similar to performing BO with EHVI, but, instead of fitting surrogate models for each considered dimension, we provide true evaluations for the cheap objectives.

Algorithm 2: MS-EHVI

Input : expensive and cheap objectives $f = (f_{\text{exp}}, f_{\text{cheap}})$, surrogate model \hat{f}_{exp} ,
number of function evaluations n_{fe}

Output: Pareto front w.r.t. f

- 1 Initialize population \mathcal{P} with initial observations
- 2 **for** $k = 1$ **to** n_{fe} **do**
- 3 Fit surrogate model \hat{f}_{exp} on \mathcal{P}
- 4 Select next candidate: $\lambda_{\text{new}} \in \text{argmax}_{\lambda} \text{EHVI}(\lambda | \mathcal{P}, \hat{f}_{\text{exp}}, f_{\text{cheap}})$
- 5 Evaluate $f_{\text{exp}}(\lambda_{\text{new}})$
- 6 Update data: $\mathcal{P} \leftarrow \mathcal{P} \cup \{(\lambda_{\text{new}}, f(\lambda_{\text{new}}))\}$
- 7 **return** $\text{pareto_front}(\mathcal{P} | f)$

Empirical results show how our method is able to obtain an appropriate exploration of the Pareto front, effectively showing a superior performance compared to vanilla EHVI, compare Figure 4 in the appendix.

3.4 MO-BANANAS

BANANAS (White et al., 2019) uses an ensemble of neural networks for predicting the performance of a neural network within BO in combination with a novel path-based encoding.

Given a set of already evaluated candidates, the best one is chosen and mutated to generate new candidates. These candidates are evaluated by means of the predictor, and the resulting predictions are used to determine the next candidate for evaluation in combination with an acquisition function as usual in BO.

To extend BANANAS for multi-objective optimization, we create a Pareto front from the predictions for the objective function values and sort according to crowd sorting (Raquel and Naval Jr, 2005). Subsequently, the next architectures are drawn from this ranking by means of independent Thompson sampling for evaluation, which works best for candidate selection according to White et al. (2019). In the same way, parent architectures are selected for generating new candidates through mutations by first forming a Pareto front and then sorting it using crowd sorting, see Algorithm 3.

Note that we do not use the path-based encoding from White et al. (2019) since it is not meaningful for our search space. Rather, we employ a simple real-valued vector representation, which furthermore also directly allows us to include non-architectural hyperparameters. We employ Gaussian noise for mutating parents: We assume integer-valued hyperparameters (e.g., number of layers), and normalize each value by dividing by the maximum value to map each hyperparameter to the range $[0, 1]$: we then add Gaussian noise. Before each function evaluation, this continuous representation is discretized by choosing the integer-valued hyperparameter which is closed to the mutation value after normalization.

Algorithm 3: MO-BANANAS

Input : neural predictor \hat{f} , number of candidates to mutate n_{mut} , mutation variance σ^2 , number of new candidates n_{new} , objectives f

Output: Pareto front w.r.t. f

- 1 Generate initial population \mathcal{P}
- 2 **for** $i = 1$ **to** n **do**
- 3 train neural predictor \hat{f} on \mathcal{P}
- 4 sort \mathcal{P} using $\text{NDS}(\mathcal{P})$ and $\text{crowdingDistance}(\mathcal{P})$
- 5 choose top- n_{mut} candidates from \mathcal{P} and **mutate** by adding noise $\eta \sim \mathcal{N}(0, \sigma^2)$ (drawn independently for each dimension of the candidates)
- 6 evaluate chosen n_{mut} candidates using \hat{f}
- 7 choose top- n_{new} candidates $\lambda_1, \dots, \lambda_{n_{\text{new}}}$ via independent Thompson sampling
- 8 evaluate $f(\lambda_1), \dots, f(\lambda_{n_{\text{new}}})$ $\mathcal{P} \leftarrow \mathcal{P} \cup \{(\lambda_1, f(\lambda_1)), \dots, (\lambda_{n_{\text{new}}}, f(\lambda_{n_{\text{new}}}))\}$
- 9 **return** $\text{pareto_front}(\mathcal{P}|f)$

This approach can be further extended by successive halving to quickly discard poorly performing architectures chosen by the neural predictor. In the experimental section we employ this version of MO-BANANAS since we empirically found it to yield improved performance.

3.5 BULK & CUT

BULK & CUT combines a very simple evolutionary strategy with BO. The name BULK & CUT comes from the fact that the algorithm first looks for high accuracy models by successively

enlarging them with network morphisms (Chen et al., 2015), then shrinking them using pruning techniques in combination with knowledge distillation (Hinton et al., 2015). A BULK & CUT run comprises three sequential phases:

1. Initialization: sample random architectures and train them;
2. Bulk-up: generate offsprings by applying network morphisms;
3. Cut-down: prune bulked-up models.

After the initialization phase is completed, parents are selected for the bulk-up phase. For this, we propose the *Parepsilon Greedy* criterion, which combines non-dominated sorting and an ϵ -greedy exploration strategy, as described in Algorithm 4. This criterion attributes a non-zero chance for being a parent to all models from the initialization phase. However, the chance of selection is higher for individuals in fronts closer to the Pareto Front. Individuals from the same front are selected with equal probability.

Algorithm 4: Parepsilon greedy

Input : Population \mathcal{P} , exploration probability ϵ
Output: $\lambda \in \mathcal{P}$

```

1 while True do
2    $\mathcal{F} \leftarrow \text{pareto\_front}(\mathcal{P});$ 
3   if  $\text{rand}() \leq 1 - \epsilon$  or  $\mathcal{F} == \mathcal{P}$  then
4     Sample  $\lambda$  from  $\mathcal{F}$ ;
5     return  $\lambda$ ;
6   else
7      $\mathcal{P} \leftarrow \mathcal{P} \setminus \mathcal{F};$ 

```

Once a parent is chosen, an offspring is generated by applying a network morphism. Network morphisms are commonly employed as mutations in the NAS literature since they avoid retraining from scratch by inheriting the knowledge of the parent (Elsken et al., 2017, 2019a; Schorn et al., 2020; Cai et al., 2018). In our experiments, two morphism operators are implemented: insert a convolutional layer and insert a fully-connected layer, at random positions.

In the cut-down phase, we employ pruning techniques to shrink models from the first two phases. We use structured pruning (Anwar et al., 2017) in our experiments, i.e., eliminating units from fully-connected layers and filters from convolutional layers, instead of dropping individual weights.

The units/filters were ranked by the sum of their output weights, and those on the bottom of the list were pruned.

We employ knowledge distillation (Hinton et al., 2015) for training the shrunken models so that they match their parent’s output (Elsken et al., 2019a; Prakosa et al., 2020; Chen et al., 2021). Note that in the evaluation phase of these models, there is no more training and the shrunk models are not fine-tuned on training labels.

During all three phases, the non-architectural hyperparameters (e.g., learning rate and weight decay) are optimized via constrained BO. The term *constrained* here refers to the fact that the optimization of the acquisition function is performed with constraints on all architectural hyperparameters, since they have already been specified, as previously explained. Note that the surrogate model still covers the architectural hyperparameters; thus it is still aware of them and the surrogate model is fitted and shared across architectures.

Algorithm 5 summarizes how BULK & CUT works.

Algorithm 5: BULK & CUT

Input : time budgets $T_1 < T_2 < T_3$, exploration probability ϵ , objectives f
Output: set of Pareto optimal solutions

- 1 $\mathcal{P} \leftarrow \emptyset$ //population set
- 2 $t \leftarrow elapsed_time()$
- 3 **while** $t < T_3$ **do**
- 4 **if** $t \in [0, T_1)$ **then**
- 5 $\lambda_\alpha \leftarrow random_architecture()$
- 6 **if** $t \in [T_1, T_2)$ **then**
- 7 $\lambda_\alpha \leftarrow paretsilon_greedy(\mathcal{P}, \epsilon)$ /* parent selection (see Alg. 4) */
- 8 $\lambda_\alpha \leftarrow network_morphism(\lambda_\alpha)$
- 9 **if** $t \in [T_2, T_3]$ **then**
- 10 $\lambda_\alpha \leftarrow paretsilon_greedy(\mathcal{P}, \epsilon)$ /* parent selection (see Alg. 4) */
- 11 $\lambda_\alpha \leftarrow prune_and_distill_knowledge(\lambda_\alpha)$
- 12 $\lambda_\beta \leftarrow constrained_BO(\lambda_\alpha)$ /* other hyperparameters */
- 13 evaluate $f(\lambda_\alpha, \lambda_\beta)$
- 14 Update *constrained_BO* with $(\lambda_\alpha, \lambda_\beta, f(\lambda_\alpha, \lambda_\beta))$
- 15 $\mathcal{P} \leftarrow \mathcal{P} \cup \{(\lambda_\alpha, \lambda_\beta, f(\lambda_\alpha, \lambda_\beta))\}$
- 16 $t \leftarrow elapsed_time()$
- 17 **return** *pareto_front*(\mathcal{P})

4. Experiments

We start by describing our experimental setup in Section 4.1 and present results in Section 4.2.

4.1 Experimental Setup

Each of the proposed methods, along with random search as the simplest baseline, is run 10 times on each dataset, with a runtime limit of 24 hours (per run and per method) on a single RTX 2080 Ti GPU.

A maximum budget of 25 epochs for training a single configuration is defined, although it is up to the methods to decide if they want to train with a smaller budget to speed up the search. We target network size (by means of number of parameters) and classification accuracy as the objectives of our multi-objective optimization.

Hyperparameter	Range	Log scale
Num. convolutional layers	{1, 2, 3}	No
Num. filters conv. layer i	$[2^4, 2^{10}]$	Yes
Kernel size	{3, 5, 7}	No
Batch normalization	{ <i>true</i> , <i>false</i> }	No
Global average pooling	{ <i>true</i> , <i>false</i> }	No
Num. fully connected layers	{1, 2, 3}	No
Num. neurons FC layer i	$[2^1, 2^9]$	Yes
Learning rate	$[10^{-5}, 10^0]$	Yes
Batch size	$[2^0, 2^9]$	Yes

Table 2: Joint space of architectural and non-architectural hyperparameters being optimized.

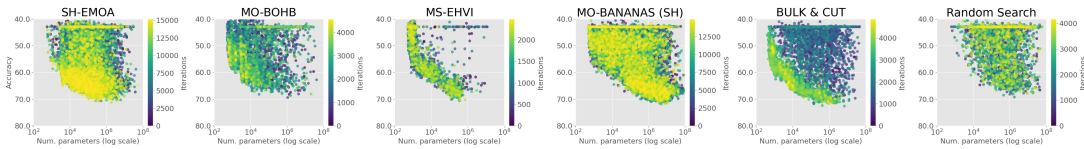
Datasets. We used the Oxford-Flowers dataset (Nilsback and Zisserman, 2006), a small dataset composed of 17 different classes with 80 examples each, to show the performance of the proposed approaches in environments where many, cheap function evaluations are available. All images are scaled down to a resolution of 16×16 for computational reasons. We also tested our methods on Fashion MNIST (Xiao et al., 2017). We split the datasets as follows: for Flowers, we randomly split the data into 60% for training, 20% for validation and 20% for testing. For Fashion-MNIST, we split the train set as defined in PyTorch into training (80%) and validation (20%) and use the original test split for testing. Neural network weights are always trained on training data, their performance on validation data is used to guide hyperparameter and architecture optimization, and the test set is only used for evaluation.

Search Space. As both target datasets are composed of images as input, all architectures start with a variable number of convolutional layers, with a variable number of filters for each layer and a variable kernel size. All layers employ ReLU activation functions, followed by max-pooling to reduce spatial dimensions. Batch normalization may be chosen after each layer. After the last convolution, a global average pooling may be applied. The feature volume is flattened and fed to a variable-length sequence of fully connected layers, with a variable number of neurons and using ReLU as the activation function. After the last hidden layer, a final fully connected layers maps to the class predictions. We always use Adam (Kingma and Ba, 2015) to optimize neural network weights, with a searchable learning rate and batch size. The number of filters of the convolutional layers, the number of neurons on the hidden layers, the learning rate, and the batch size are considered on a logarithmic scale.

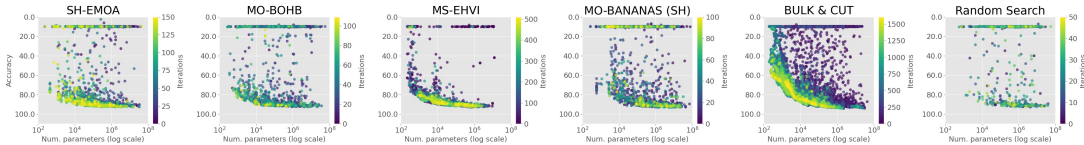
We refer to Table 2 for a summary of our search space.

4.2 Results

Visualizing sampled configurations. Figure 1 visualizes the sampled configurations for each method across all 10 random seeds.



(a) Sampled configurations for each method on Flowers. We only show a random subset of 10% of all sampled points for visualization purposes.



(b) Sampled configurations on Fashion-MNIST dataset.

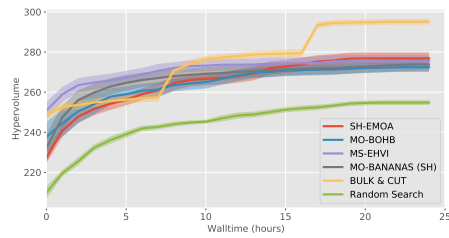
Figure 1: Sampled configurations for each method on Fashion-MNIST.

For the Flowers dataset (upper row), all methods (except random search) explore the Pareto front, which is what they were designed for. However, they also significantly differ in the exploration strategy. SH-EMOA explores both objective functions equally well but still samples poor configurations in later iterations. MO-BOHB tends to focus on smaller networks in later iterations, while MS-EHVI very quickly discovers networks close to the Pareto front and mostly samples new configurations there. After an initial phase, BULK & CUT also mostly samples candidates close to the Pareto front in later iterations. For Fashion-MNIST, already very small networks yield a high accuracy, making it hard to actually trade-off the different objective functions. However, one can still see that all methods focus on promising regions in objective function space.

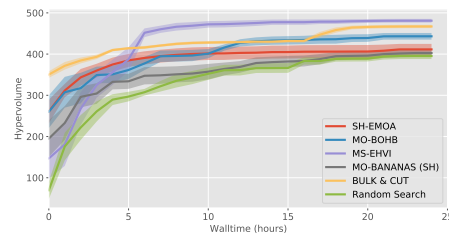
Anytime performance over the course of multi-objective joint NAS+HPO. Figure 2 shows the hypervolume indicator over time, averaged across the 10 independent runs per method on each of the two datasets. All our methods clearly outperform random search. For Flowers, MS-EHVI converges very fast but is eventually outperformed by BULK & CUT, which however performs less strongly in the initial phase. SH-EMOA, MO-BOHB and MO-BANANAS perform similarly. For Fashion-MNIST, MS-EHVI and BULK & CUT again slightly outperform the remaining approaches.

Final results. Figure 3 shows the final Pareto fronts for all methods when combining the results from all seeds.

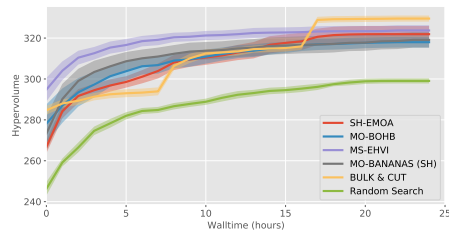
The proposed methods perform similarly for the range of parameters from 10^3 to 10^5 , but some methods have problems with covering smaller or larger models. When looking at results for each seed other runs (please refer to Figures 5 and 6 in the appendix), we however also noticed that the results vary across seeds, indicating that initializing might have a high impact on the performance and that the budget of 24 hours might not be sufficient for the methods to converge or that methods simply get stuck in a local optimum. Table 3 summarizes the obtained hypervolume of the final Pareto front for each method.



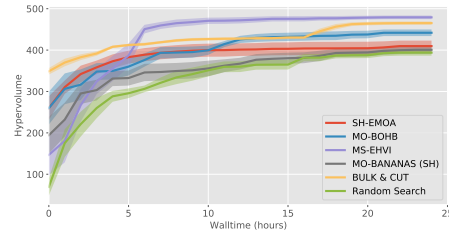
(a) Flowers dataset on validation split.



(b) Fashion-MNIST dataset on validation split.

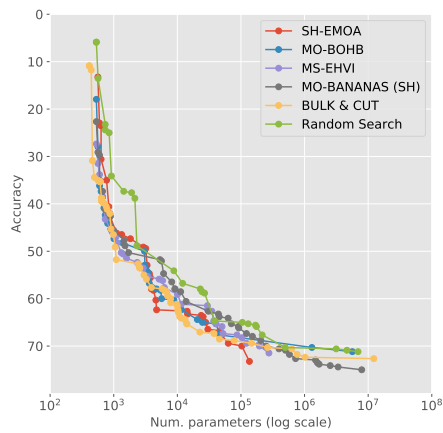


(c) Flowers dataset on test split.

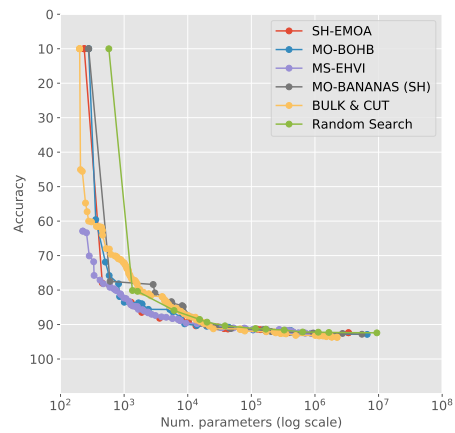


(d) Fashion-MNIST dataset on test split.

Figure 2: Hypervolume obtained by the different methods over time. We show means \pm standard errors of the mean based on 10 independent runs of each method.



(a) Pareto fronts on Flowers dataset.



(b) Pareto fronts on Fashion-MNIST dataset.

Figure 3: Pareto fronts by combining the results of the 10 different runs for each method on the test split

	Hypervolume (mean \pm std. error)	
	Flowers	Fashion-MNIST
Random search	299.05 \pm 1.19	393.86 \pm 6.97
SH-EMOA	321.90 \pm 3.79	409.61 \pm 12.61
MO-BOHB	317.98 \pm 2.48	441.86 \pm 7.58
MS-EHVI	323.72 \pm 2.46	479.13 \pm 4.15
MO-BANANAS	319.11 \pm 3.59	400.71 \pm 9.00
BULK & CUT	329.54 \pm 1.41	465.19 \pm 3.83

Table 3: Final hypervolume obtained by each method on both test datasets. We show means \pm standard errors based on 10 independent runs.

5. Conclusions

We addressed the problem of joint hyperparameter optimization and neural architecture search under multiple objectives by extending existing methods to this scenario. We recommend that the proposed methods serve as baselines for future research in this direction. To facilitate this, all our code is available under <https://github.com/automl/multi-obj-baselines> under a permissive Open Source license (Apache 2.0).

Acknowledgments

The authors acknowledge funding by the Robert Bosch GmbH. A part of this work was supported by the German Federal Ministry of Education and Research (BMBF, grant RenormalizedFlows 01IS19077C).

References

- Sajid Anwar, Kyuyeon Hwang, and Wonyong Sung. Structured pruning of deep convolutional neural networks. *13(3)*, 2017.
- Johannes Bader and Eckart Zitzler. Hype: An algorithm for fast hypervolume-based many-objective optimization. *Evolutionary computation*, 19(1):45–76, 2011.
- Gabriel Bender, Pieter-Jan Kindermans, Barret Zoph, Vijay Vasudevan, and Quoc Le. Understanding and simplifying one-shot architecture search. In *International Conference on Machine Learning*, 2018.
- Hadjer Benmeziane, Kaoutar El Maghraoui, Hamza Ouarnoughi, Smail Niar, Martin Wis-tuba, and Naigang Wang. A comprehensive survey on hardware-aware neural architecture search, 2021.
- J. Bergstra, R. Bardenet, Y. Bengio, and B. Kégl. Algorithms for hyper-parameter optimization. In J. Shawe-Taylor, R. Zemel, P. Bartlett, F. Pereira, and K. Weinberger, editors, *Proceedings of the 25th International Conference on Advances in Neural Information Processing Systems (NeurIPS’11)*, pages 2546–2554, 2011.
- Nicola Beume, Boris Naujoks, and Michael Emmerich. SMS-EMOA: Multiobjective selection based on dominated hypervolume. *European Journal of Operational Research*, 181(3):1653–1669, 2007.
- E. Brochu, V. Cora, and N. de Freitas. A tutorial on Bayesian optimization of expensive cost functions, with application to active user modeling and hierarchical reinforcement learning. *arXiv:1012.2599v1 [cs.LG]*, 2010.
- Han Cai, Tianyao Chen, Weinan Zhang, Yong Yu, and Jun Wang. Efficient architecture search by network transformation. In *Association for the Advancement of Artificial Intelligence*, 2018.
- Han Cai, Ligeng Zhu, and Song Han. ProxylessNAS: Direct neural architecture search on target task and hardware. In *International Conference on Learning Representations*, 2019.
- Liyang Chen, Yongquan Chen, Juntong Xi, and Xinyi Le. Knowledge from the original network: restore a better pruned network with knowledge distillation. *Complex and Intelligent Systems*, 01 2021.
- Tianqi Chen, Ian Goodfellow, and Jonathon Shlens. Net2net: Accelerating learning via knowledge transfer. *arXiv preprint arXiv:1511.05641*, 2015.
- Samuel Daulton, Maximilian Balandat, and Eytan Bakshy. Differentiable expected hypervolume improvement for parallel multi-objective bayesian optimization. *arXiv preprint arXiv:2006.05078*, 2020.
- K. Deb, A. Pratap, S. Agarwal, and T. Meyarivan. A Fast and Elitist Multiobjective Genetic Algorithm: NSGA-II. *Trans. Evol. Comp.*, 6(2), April 2002.

- Kalyanmoy Deb. *Multi-Objective Evolutionary Algorithms*, pages 995–1015. Springer Berlin Heidelberg, Berlin, Heidelberg, 2015. ISBN 978-3-662-43505-2. doi: 10.1007/978-3-662-43505-2_49. URL https://doi.org/10.1007/978-3-662-43505-2_49.
- T. Domhan, J. Springenberg, and F. Hutter. Speeding up automatic hyperparameter optimization of deep neural networks by extrapolation of learning curves. In Q. Yang and M. Wooldridge, editors, *Proceedings of the 25th International Joint Conference on Artificial Intelligence (IJCAI’15)*, pages 3460–3468, 2015.
- Xuanyi Dong, Mingxing Tan, Adams Wei Yu, Daiyi Peng, Bogdan Gabrys, and Quoc V. Le. Autohas: Differentiable hyper-parameter and architecture search. *arXiv preprint*, 2020.
- Thomas Elsken, Jan Hendrik Metzen, and Frank Hutter. Simple And Efficient Architecture Search for Convolutional Neural Networks. In *NeurIPS Workshop on Meta-Learning*, 2017.
- Thomas Elsken, Jan Hendrik Metzen, and Frank Hutter. Efficient multi-objective neural architecture search via lamarckian evolution. In *International Conference on Learning Representations*, 2019a.
- Thomas Elsken, Jan Hendrik Metzen, and Frank Hutter. Neural architecture search: A survey. *Journal of Machine Learning Research*, 20(55):1–21, 2019b.
- Michael Emmerich. Single-and multi-objective evolutionary design optimization assisted by gaussian random field metamodels. *University of Dortmund*, 2005.
- Michael Emmerich, Nicola Beume, and Boris Naujoks. An emo algorithm using the hypervolume measure as selection criterion. In Carlos A. Coello Coello, Arturo Hernández Aguirre, and Eckart Zitzler, editors, *Evolutionary Multi-Criterion Optimization*, pages 62–76, Berlin, Heidelberg, 2005. Springer Berlin Heidelberg. ISBN 978-3-540-31880-4.
- D. Eriksson, M. Pearce, J. R. Gardner, R. Turner, and M. Poloczek. Scalable global optimization via local bayesian optimization. In H. Wallach, H. Larochelle, A. Beygelzimer, F. d’Alché-Buc, E. Fox, and R. Garnett, editors, *Proceedings of the 33rd International Conference on Advances in Neural Information Processing Systems (NeurIPS’19)*, 2019.
- S. Falkner, A. Klein, and F. Hutter. BOHB: Robust and efficient hyperparameter optimization at scale. In J. Dy and A. Krause, editors, *Proceedings of the 35th International Conference on Machine Learning (ICML’18)*, volume 80, pages 1437–1446. Proceedings of Machine Learning Research, 2018.
- M. Feurer, J. Springenberg, and F. Hutter. Initializing Bayesian hyperparameter optimization via meta-learning. In B. Bonet and S. Koenig, editors, *Proceedings of the Twenty-ninth National Conference on Artificial Intelligence (AAAI’15)*, pages 1128–1135. AAAI Press, 2015.

- Matthias Feurer and Frank Hutter. Hyperparameter optimization. In Frank Hutter, Lars Kotthoff, and Joaquin Vanschoren, editors, *AutoML: Methods, Systems, Challenges*, chapter 1, pages 3–33. Springer, May 2019.
- Xavier Gastaldi. Shake-shake regularization. In *International Conference on Learning Representations Workshop*, 2017.
- Geoffrey Hinton, Oriol Vinyals, and Jeff Dean. Distilling the knowledge in a neural network. *arXiv preprint arXiv:1503.02531*, 2015.
- F. Hutter, H. Hoos, and K. Leyton-Brown. Sequential model-based optimization for general algorithm configuration. In C. Coello, editor, *Proceedings of the Fifth International Conference on Learning and Intelligent Optimization (LION'11)*, volume 6683 of *Lecture Notes in Computer Science*, pages 507–523. Springer, 2011.
- Kevin Jamieson and Ameet Talwalkar. Non-stochastic best arm identification and hyperparameter optimization. In *Artificial Intelligence and Statistics*, pages 240–248. PMLR, 2016.
- K. Kandasamy, K. R. Vysyaraju, W. Neiswanger, B. Paria, C. R. Collins, J. Schneider, B. Póczos, and E. P. Xing. Tuning hyperparameters without grad students: Scalable and robust bayesian optimisation with dragonfly. *Journal of Machine Learning Research*, 21(81):1–27, 2020. URL <http://jmlr.org/papers/v21/18-223.html>.
- Kirthevasan Kandasamy, Willie Neiswanger, Jeff Schneider, Barnabas Póczos, and Eric P Xing. Neural architecture search with bayesian optimisation and optimal transport. In *Advances in Neural Information Processing Systems 31*. 2018.
- D. Kingma and J. Ba. Adam: A method for stochastic optimization. In *Proceedings of the International Conference on Learning Representations (ICLR'15)*, 2015. Published online: iclr.cc.
- A. Klein, S. Falkner, S. Bartels, P. Hennig, and F. Hutter. Fast Bayesian optimization of machine learning hyperparameters on large datasets. In A. Singh and J. Zhu, editors, *Proceedings of the Seventeenth International Conference on Artificial Intelligence and Statistics (AISTATS)*, volume 54. Proceedings of Machine Learning Research, 2017.
- L. Li, K. Jamieson, G. DeSalvo, A. Rostamizadeh, and A. Talwalkar. Hyperband: A novel bandit-based approach to hyperparameter optimization. *Journal of Machine Learning Research*, 18(185):1–52, 2018.
- Hanxiao Liu, Karen Simonyan, and Yiming Yang. DARTS: Differentiable architecture search. In *International Conference on Learning Representations*, 2019.
- Zhichao Lu, Ian Whalen, Vishnu Boddeti, Yashesh Dhebar, Kalyanmoy Deb, Erik Goodman, and Wolfgang Banzhaf. NSGA-net: A multi-objective genetic algorithm for neural architecture search, 2019.
- H. Mendoza, A. Klein, M. Feurer, J. Springenberg, and F. Hutter. Towards automatically-tuned neural networks. In *ICML 2016 AutoML Workshop*, 2016.

- Kaisa Miettinen. *Nonlinear Multiobjective Optimization*. Springer Science & Business Media, 1999.
- Jonas Moćkus. On bayesian methods for seeking the extremum. In *Optimization techniques IFIP technical conference*, pages 400–404. Springer, 1975.
- Maria-Elena Nilsback and Andrew Zisserman. A visual vocabulary for flower classification. In *IEEE Conference on Computer Vision and Pattern Recognition*, volume 2, pages 1447–1454, 2006.
- Yoshihiko Ozaki, Yuki Tanigaki, Shuhei Watanabe, and Masaki Onishi. Multiobjective tree-structured parzen estimator for computationally expensive optimization problems. In *Proceedings of the 2020 Genetic and Evolutionary Computation Conference*, pages 533–541, 2020.
- Hieu Pham, Melody Y. Guan, Barret Zoph, Quoc V. Le, and Jeff Dean. Efficient neural architecture search via parameter sharing. In *International Conference on Machine Learning*, 2018.
- S. W. Prakosa, J. Leu, and Zhaohong Chen. Improving the accuracy of pruned network using knowledge distillation. *Pattern Analysis and Applications*, pages 1–12, 2020.
- Carlo R Raquel and Prospero C Naval Jr. An effective use of crowding distance in multi-objective particle swarm optimization. In *Proceedings of the 7th Annual conference on Genetic and Evolutionary Computation*, pages 257–264, 2005.
- C. Rasmussen and C. Williams. *Gaussian Processes for Machine Learning*. The MIT Press, 2006.
- Esteban Real, Sherry Moore, Andrew Selle, Saurabh Saxena, Yutaka Leon Suematsu, Jie Tan, Quoc V. Le, and Alexey Kurakin. Large-scale evolution of image classifiers. In Doina Precup and Yee Whye Teh, editors, *Proceedings of the 34th International Conference on Machine Learning*, volume 70 of *Proceedings of Machine Learning Research*, pages 2902–2911, International Convention Centre, Sydney, Australia, 06–11 Aug 2017. PMLR.
- Esteban Real, Alok Aggarwal, Yanping Huang, and Quoc V. Le. Aging Evolution for Image Classifier Architecture Search. In *AAAI*, 2019.
- Frederic Runge, Danny Stoll, Stefan Falkner, and Frank Hutter. Learning to design RNA. In *International Conference on Learning Representations*, 2019.
- T. Saikia, Y. Marrakchi, A. Zela, F. Hutter, and T. Brox. Autodispnet: Improving disparity estimation with automl. In *IEEE International Conference on Computer Vision (ICCV)*, October 2019.
- Christoph Schorn, Thomas Elsken, Sebastian Vogel, Armin Runge, Andre Guntoro, and Gerd Ascheid. Automated design of error-resilient and hardware-efficient deep neural networks. *Neural Computing and Applications*, pages 1 – 19, 2020.

- B. Shahriari, K. Swersky, Z. Wang, R. Adams, and N. de Freitas. Taking the human out of the loop: A review of Bayesian optimization. *Proceedings of the IEEE*, 104(1):148–175, 2016.
- J. Snoek, H. Larochelle, and R. Adams. Practical Bayesian optimization of machine learning algorithms. In P. Bartlett, F. Pereira, C. Burges, L. Bottou, and K. Weinberger, editors, *Proceedings of the 26th International Conference on Advances in Neural Information Processing Systems (NeurIPS’12)*, pages 2960–2968, 2012.
- J. Snoek, K. Swersky, R. Zemel, and R. Adams. Input warping for Bayesian optimization of non-stationary functions. In E. Xing and T. Jebara, editors, *Proceedings of the 31th International Conference on Machine Learning, (ICML’14)*, pages 1674–1682. Omnipress, 2014.
- J. Springenberg, A. Klein, S. Falkner, and F. Hutter. Bayesian optimization with robust Bayesian neural networks. In D. Lee, M. Sugiyama, U. von Luxburg, I. Guyon, and R. Garnett, editors, *Proceedings of the 30th International Conference on Advances in Neural Information Processing Systems (NeurIPS’16)*, 2016.
- N. Srinivas and K. Deb. Multiobjective optimization using nondominated sorting in genetic algorithms. *Evolutionary Computation*, 2(3):221–248, 1994. doi: 10.1162/evco.1994.2.3.221.
- Mingxing Tan, Bo Chen, Ruoming Pang, Vijay Vasudevan, Mark Sandler, Andrew Howard, and Quoc V. Le. Mnasnet: Platform-aware neural architecture search for mobile. In *The IEEE Conference on Computer Vision and Pattern Recognition (CVPR)*, June 2019.
- Colin White, Willie Neiswanger, and Yash Savani. Bananas: Bayesian optimization with neural architectures for neural architecture search. *arXiv preprint arXiv:1910.11858*, 2019.
- Martin Wistuba, Amrith Rawat, and Tejaswini Pedapati. A survey on neural architecture search. *arXiv preprint*, 2019.
- Han Xiao, Kashif Rasul, and Roland Vollgraf. Fashion-mnist: a novel image dataset for benchmarking machine learning algorithms, 2017.
- Kaifeng Yang, Michael Emmerich, André Deutz, and Thomas Bäck. Multi-objective bayesian global optimization using expected hypervolume improvement gradient. *Swarm and evolutionary computation*, 44:945–956, 2019.
- Arber Zela, Aaron Klein, Stefan Falkner, and Frank Hutter. Towards automated deep learning: Efficient joint neural architecture and hyperparameter search. In *ICML 2018 Workshop on AutoML (AutoML 2018)*, July 2018.
- Lucas Zimmer, Marius Lindauer, and Frank Hutter. Auto-pytorch tabular: Multi-fidelity metalearning for efficient and robust autodl. *IEEE Transactions on Pattern Analysis and Machine Intelligence*, pages 1–12, 2021. URL [Arxiv](https://arxiv.org/abs/2107.00000), [IEEEearlyaccess](https://ieeexplore.ieee.org/abstract/document/9544444). To appear.

- B. Zoph and Q. V. Le. Neural architecture search with reinforcement learning. In *Proceedings of the International Conference on Learning Representations (ICLR'17)*, 2017. Published online: [iclr.cc](https://arxiv.org/abs/1703.01564).

Appendix A. Full Details on the Various Baselines

A.1 Implementation details on SH-EMOA

- Population size and total number of samples: In Flowers dataset, we use $s_{\text{pop}} = 100$ and $n_{\text{fe}}^{\text{total}} = 15000$. In Fashion-MNIST, we use $s_{\text{pop}} = 10$ and $n_{\text{fe}}^{\text{total}} = 150$.
- Parent selection: We use tournament selection by randomly sampling k potential parents from the current population (uniform distribution) and choose the parent with highest fitness. We use $k = 3$.
- Variation: On each step we choose either mutation or recombination strategy with equal probability. Mutation is defined as a uniformly distributed random variation of 5 hyperparameters from the parent configuration. For recombination, we use two parents and choose each hyperparameter from one of them with equal probability. As we have a conditional search space, relationships between hyperparameters are taken into account when a new individual is created. For example, if a mutation increases the total number of convolutional layers, the size of the kernel for each new layer is also added.

A.2 Implementation details on MO-BOHB

Algorithms 6 and 7 show pseudo code for MO-BOHB and its sampling step, respectively. Note the close resemblance to the original BOHB (differences marked in red), as MO-BOHB generalizes BOHB to any number of objectives. Note however, that there are two minor differences between the current version of our proposed MO-BOHB and the original BOHB implementation: (i) MO-BOHB uses an hierarchy of one-dimensional KDEs, whereas BOHB use a single multi-dimensional KDE, and (ii) we do not multiply bandwidths by a constant factor b_w . In future versions of MO-BOHB, we suspect that using a single multi-dimensional KDE and multiplication of bandwidths may further improve performance by better handling interaction effects between (architectural) hyperparameters and encouraging more exploration

around promising configurations, respectively.

Algorithm 6: MO-BOHB	Algorithm 7: Sampling in MO-BOHB
<p>Input : budgets b_{min} and b_{max}, configurations discarding factor $\eta \in \mathbb{N}_{>0}$, and objectives f</p> <p>Output: Pareto front w.r.t. f</p> <ol style="list-style-type: none"> 1 $s_{max} \leftarrow \lfloor \log_{\eta} \frac{b_{max}}{b_{min}} \rfloor$ 2 $\mathcal{P}_b \leftarrow [\forall b \in \{ \eta^{-s} \cdot b_{max} \mid s = s_{max}, s_{max-1}, \dots, 0 \}$ 3 while <i>not stopping criterion</i> do 4 for $s \in \{ s_{max}, s_{max-1}, \dots, 0 \}$ do 5 sample $n = \lceil \frac{s_{max}+1}{s+1} \eta^s \rceil$ configurations $\lambda_1, \dots, \lambda_n$ using Algorithm 7 6 run modified SH on $\lambda_1, \dots, \lambda_n$ with initial budget $\eta^{-s} \cdot b_{max}$ 7 add observations $\{ (\lambda_i, f(\lambda_i)) \}$ of each budget b to \mathcal{P}_b <p>8 return <i>pareto_front</i>($\mathcal{P}_{b_{max}} \mid f$)</p>	<p>Input : observations \mathcal{P}, fraction of random runs ρ, quantile γ, number of samples n, and minimum number of points N_{min} to build a model</p> <p>Output: next configuration to evaluate</p> <ol style="list-style-type: none"> 1 if $rand() < \rho$ then 2 return random configuration 3 $b \leftarrow \arg \max \{ \mathcal{P}_b : \mathcal{P}_b \geq N_{min} + 2 \}$ 4 if $b = \emptyset$ then 5 return random configuration 6 greedily split \mathcal{P} into good \mathcal{P}_l or bad \mathcal{P}_g observations using NDS & HSSP 7 fit KDEs l and g based on \mathcal{P}_l or \mathcal{P}_g, respectively 8 draw n samples according to $l(\lambda)$ 9 return sample with highest ratio $\frac{l(\lambda)}{g(\lambda)}$

In all our experiments, we set the meta-parameters of MO-BOHB as follows: For the HB part of MO-BOHB, we set the configuration discarding factor of to $\eta = 3$, use minimum budget $b_{min} = 5$ and maximum budget $b_{max} = 25$. In the BO part of MO-BOHB, we use an random fraction $\rho = 1/6$, set the quantile to $\gamma = 0.1$, sample $n = 24$ configurations, and use a minimum of $N_{min} = 2 \cdot |HPS| + 1$ points before building a model.

A.3 Details on MS-EHVI

Figure 4 shows a comparison of MS-EHVI to standard EHVI.

Appendix B. Supplemental Results

Figures 5 and 6 show all the Pareto fronts found with different seeds.

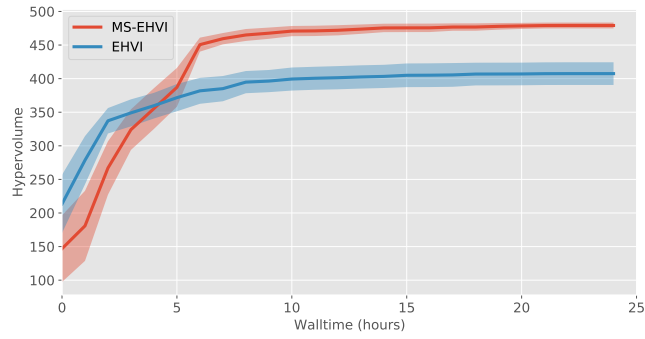


Figure 4: Comparison between EHVI and MS-EHVI on Fashion-MNIST. Hypervolume obtained by both methods over time. We show mean \pm standard error of the mean based on 10 independent runs of each method.

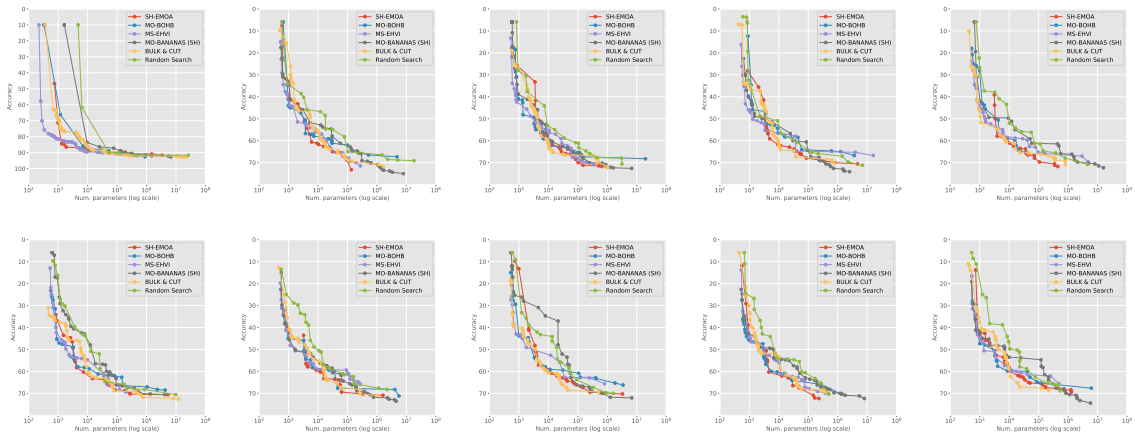


Figure 5: Pareto fronts obtained for different initial random seeds on Flowers dataset.

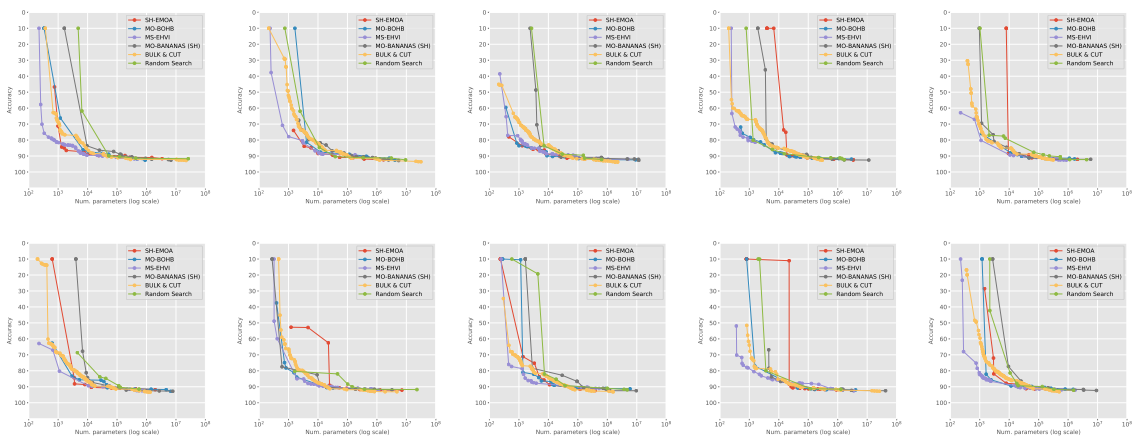


Figure 6: Pareto fronts obtained for different initial random seeds on Fashion-MNIST.